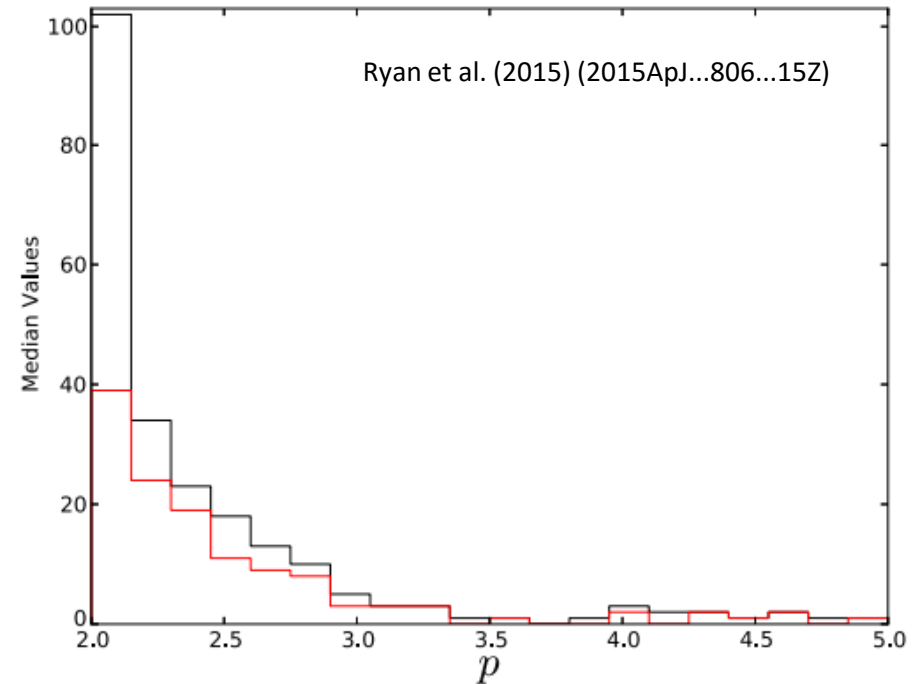


Nonlinear diffusive shock acceleration in GRB afterglows

Curran et al. (2010) (2010ApJ...716L.135C)

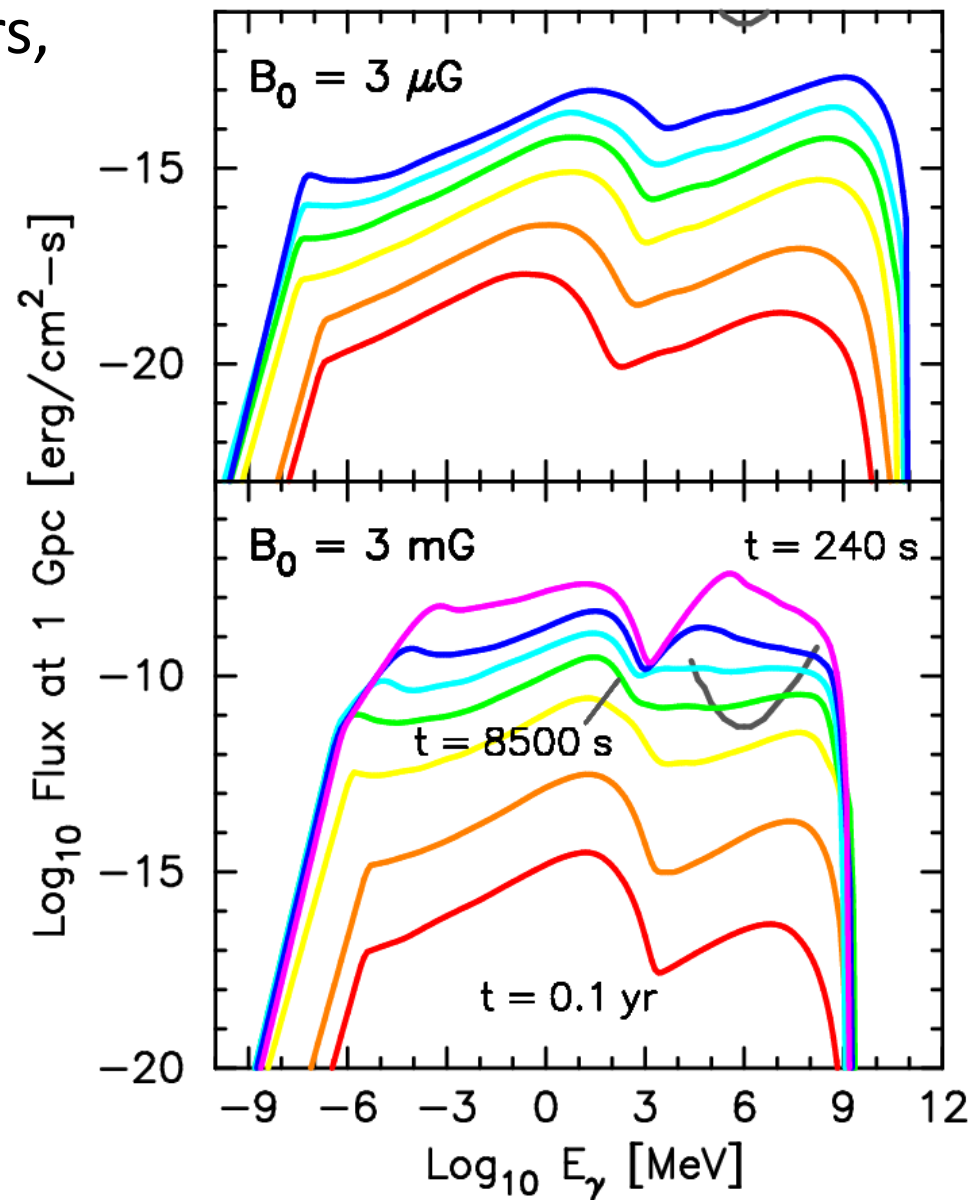
Model	p	σ_p
GDp	2.36	0.590
	(2.40 ± 0.03)	(0.600 ± 0.007)
	$[2.36 \pm 0.05]$	$[0.590 \pm 0.012]$

Notes. The most likely values of electron energy distribution index, p , the related Gaussian scatter, σ_p , the



The punchline

- For typical afterglow parameters, high-energy part of spectrum may be observable for $\approx 10^4$ s after GRB
- Detection or non-detection could serve as probe of micro-physics at shock front

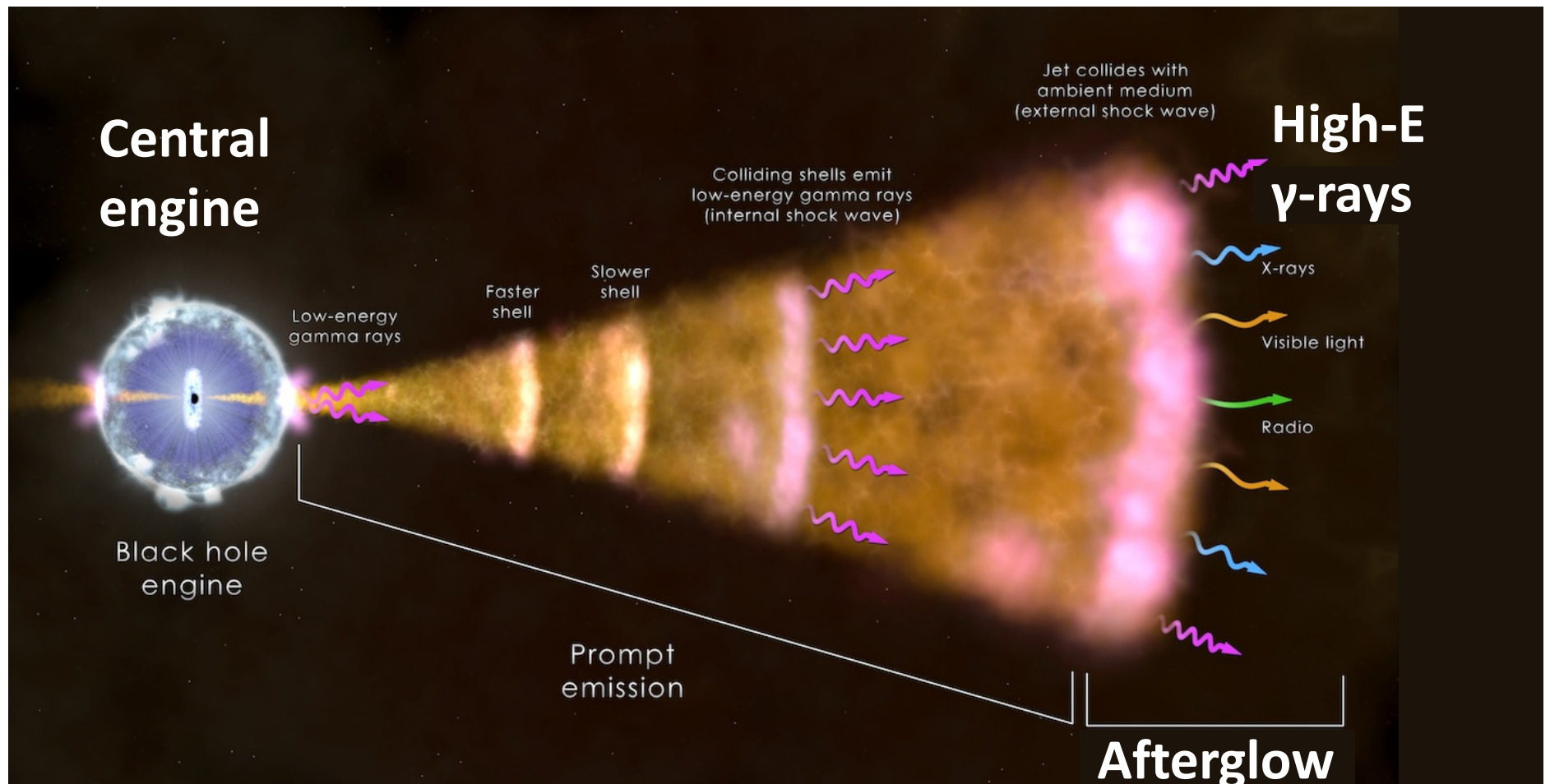


Outline

- Background
- Nonlinear diffusive shock acceleration (DSA) in relativistic shocks
- Nonlinear shock acceleration of electrons
- Afterglow observations by CTA?

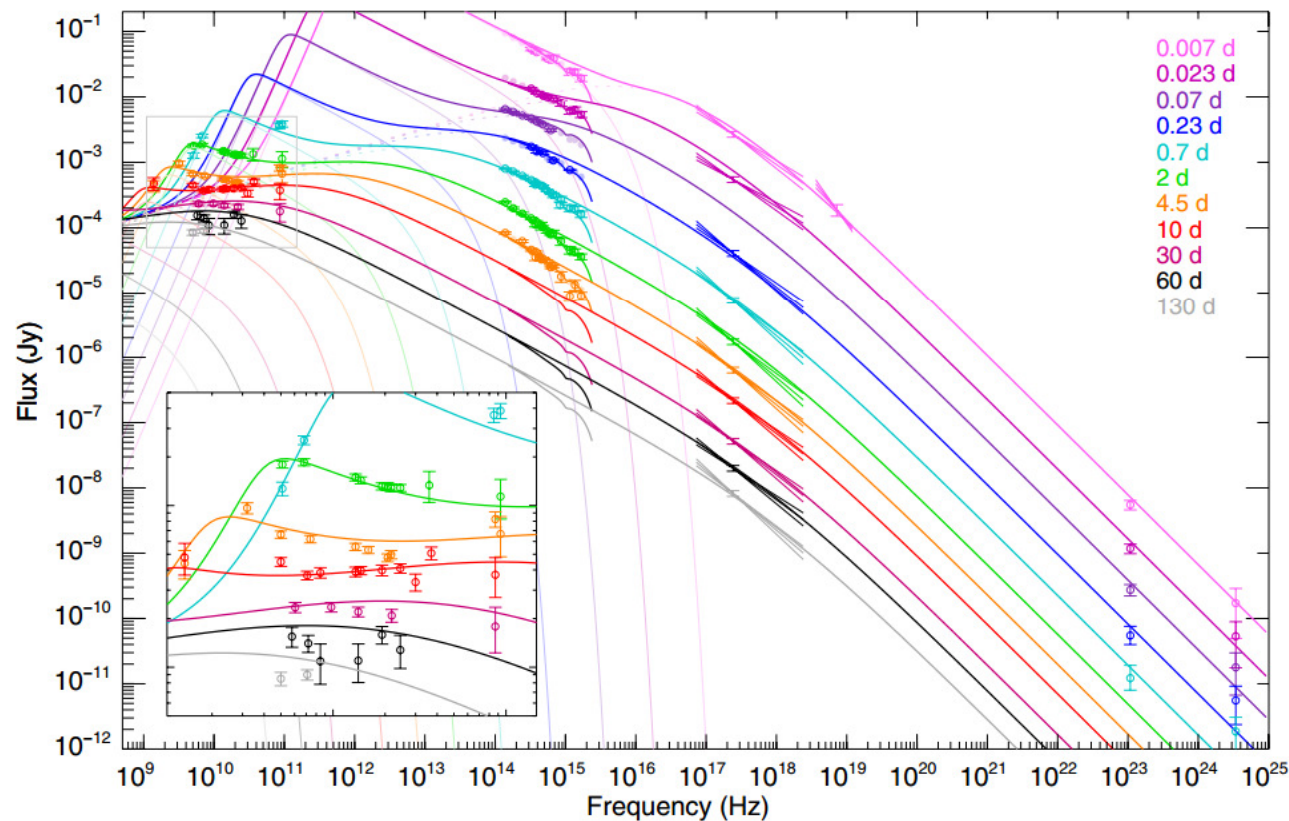
Background

Afterglow is long-lived (hours, days, months) multiwavelength relic of GRB



Background

Observations of GRB afterglows cover orders of magnitude in time and energy

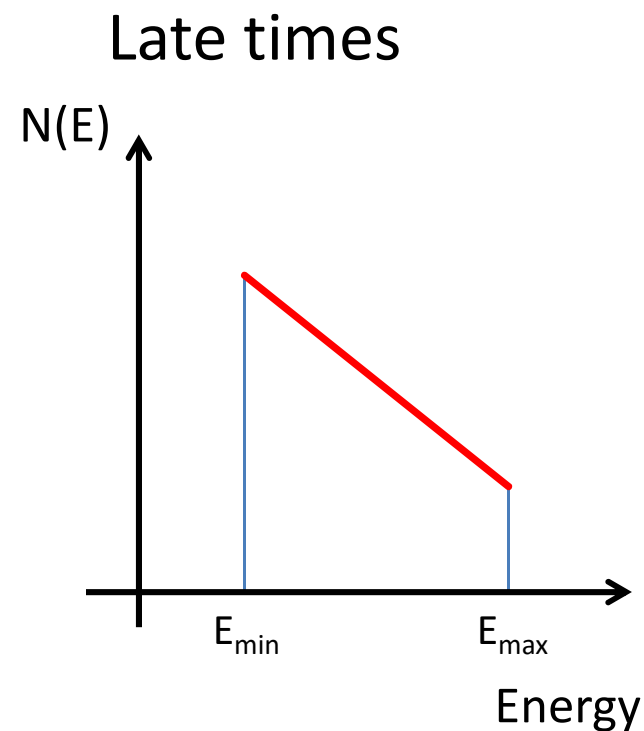
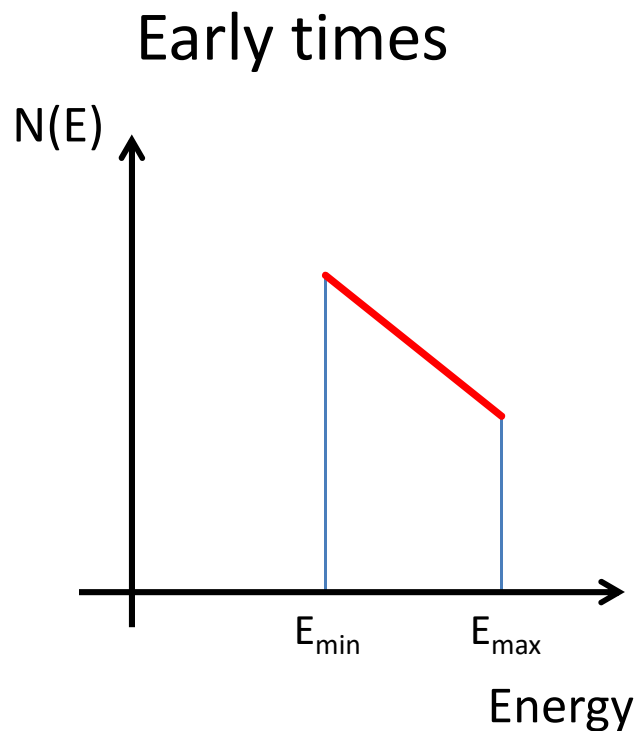


Perley et al. (2014)
(2014ApJ...781...37P)

Figure 10. Observations of the afterglow of GRB 130427A spanning from the low-frequency radio to the 100 GeV LAT bands, interpolated to a series of coeval epochs spanning from 0.007 days (10 minutes) to 130 days after the burst. Overplotted over each epoch is our simple forward+reverse shock model from standard synchrotron afterglow theory, which provides an excellent description of the entire data set, a span of 18 orders of magnitude in frequency and 4 orders of magnitude in time. The solid line shows the combined model, with the pale solid line showing the reverse-shock and the pale dotted line showing the forward-shock contribution. The “spur” at $\approx 10^{15}$ Hz shows the effects of host-galaxy extinction on the NIR/optical/UV bands. Open points with error bars are measurements (adjusted to be coeval at each epoch time); pale filled points are model optical fluxes from the empirical fit in Section 3.4. The inset at lower left shows a magnified version of the radio part of the SED (gray box) at $t > 0.7$ days.

Background

Current afterglow studies assume extremely simple model for CR electrons accelerated by shock



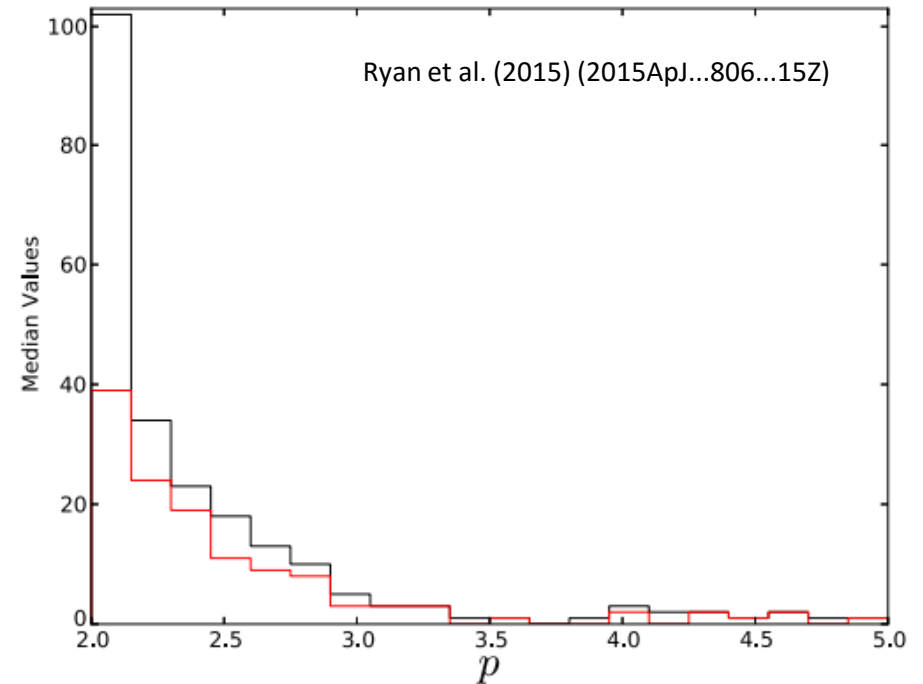
(mostly) Fine if shocks are test-particle and unaffected by B-field

Nonlinear diffusive shock acceleration in GRB afterglows

Curran et al. (2010) (2010ApJ...716L.135C)

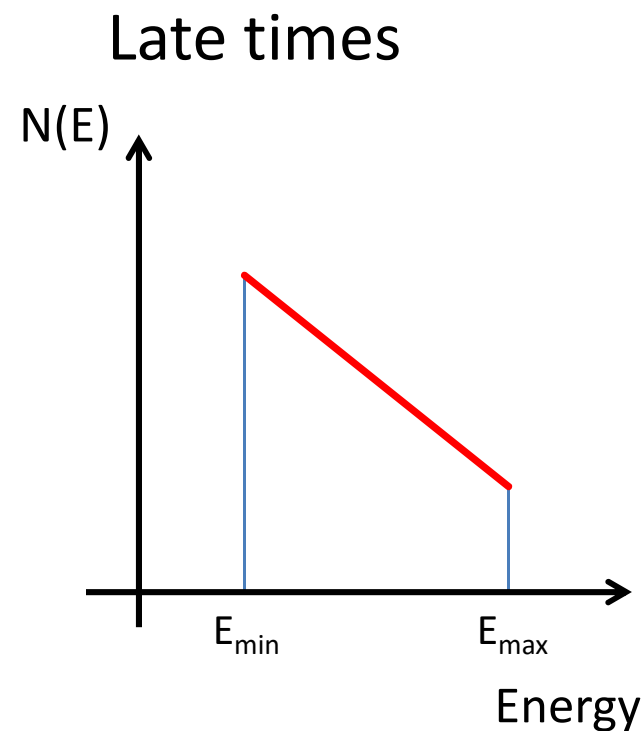
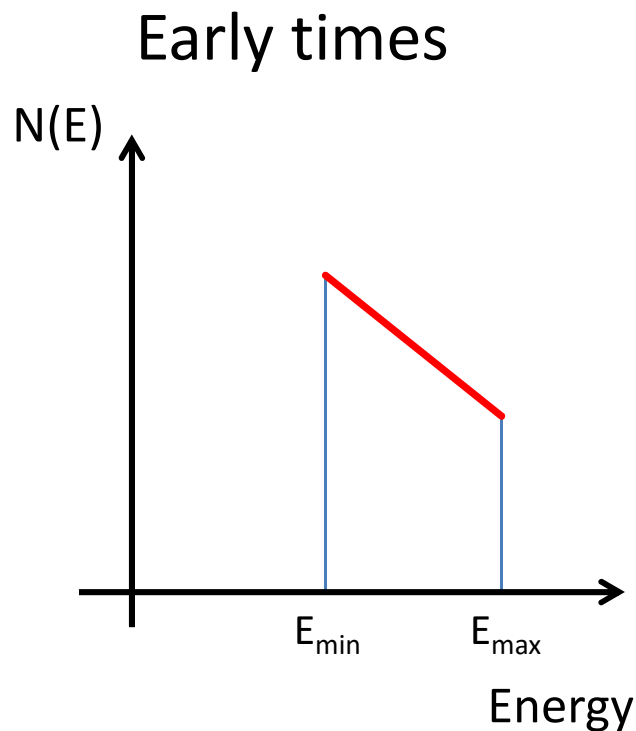
Model	p	σ_p
GDp	2.36	0.590
	(2.40 ± 0.03)	(0.600 ± 0.007)
	$[2.36 \pm 0.05]$	$[0.590 \pm 0.012]$

Notes. The most likely values of electron energy distribution index, p , the related Gaussian scatter, σ_p , the



Background

Current afterglow studies assume extremely simple model for CR electrons accelerated by shock

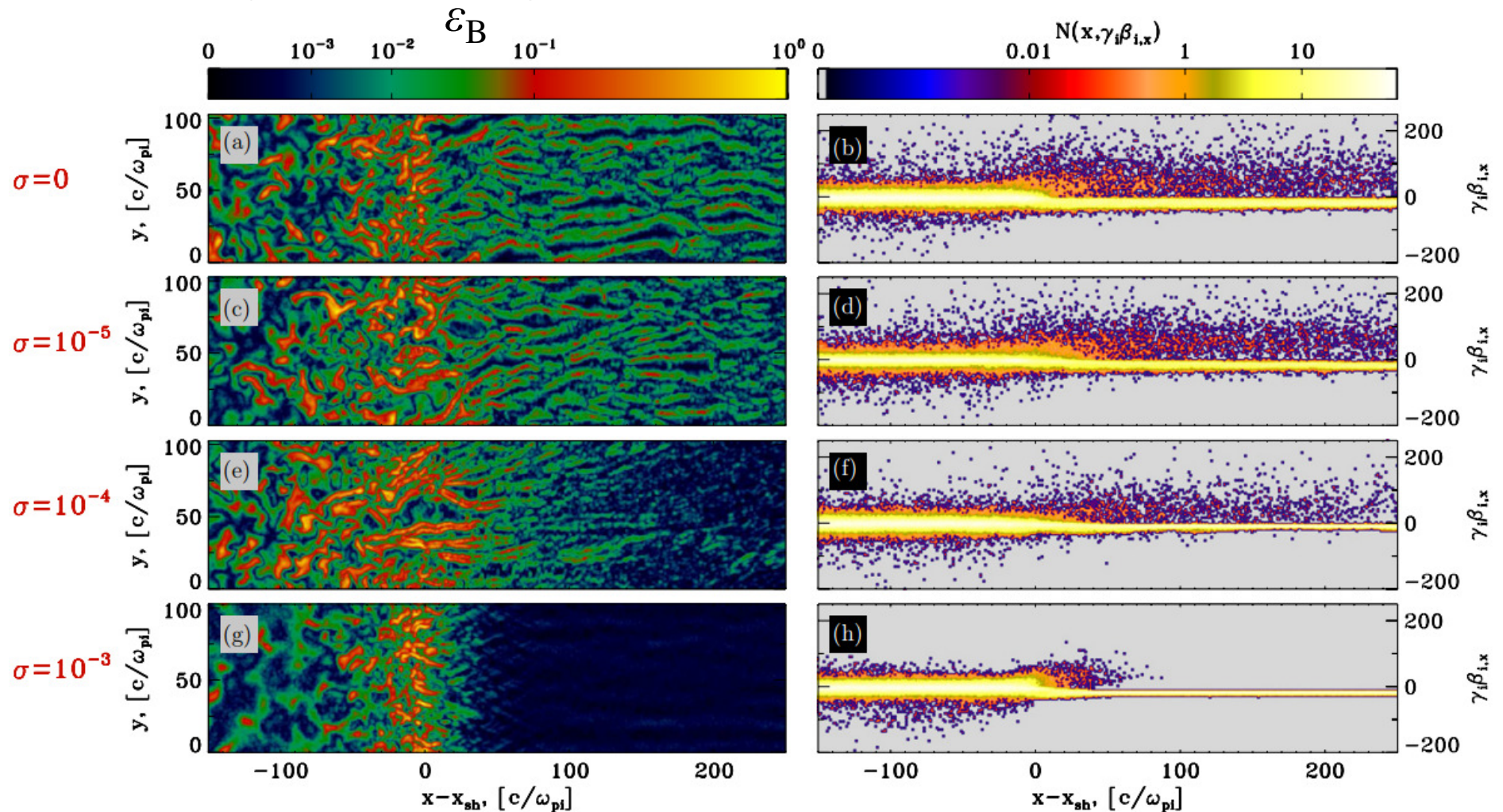


(mostly) Fine if shocks are test-particle and unaffected by B-field

Background

(Particle-in-cell)

Per PIC simulations, magnetic field may not be negligible, and accelerated particles may influence shock structure

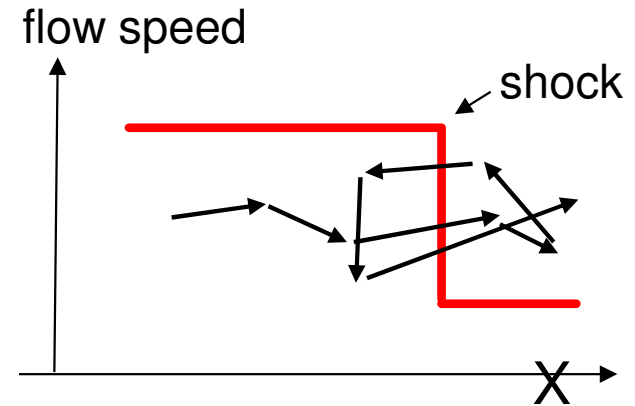
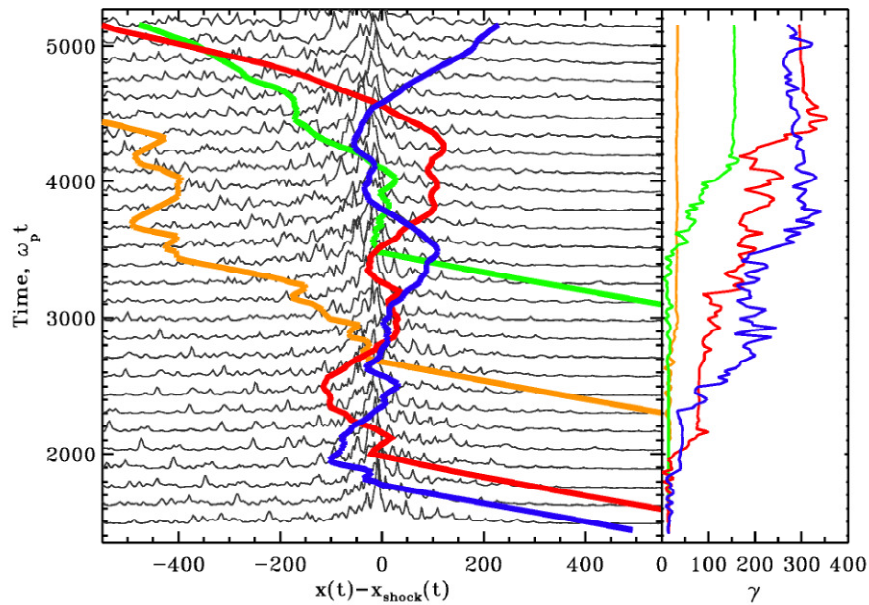


Background

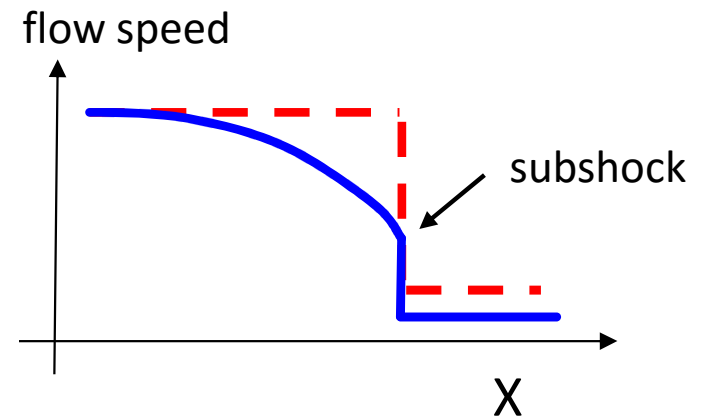
Strong B-field turbulence in vicinity of shock can scatter particles back into upstream region (\leftarrow diffusive shock acceleration, or **DSA**)

acceleration, or **DSA**)

Spitkovsky (2008) (2008ApJ...682L...5S)



Pressure from UpS particles affects inflow of plasma, which affects shock, which affects acceleration, which affects pressure from UpS particles...



Background

Interaction between shock, B-field turbulence, and accelerated particles important!

Leads to more complicated CR spectrum than simply E^{-p}

PIC simulations impractical if extended to necessary scales to model GRB afterglows

Monte Carlo approach presented here balances self-consistency & computation time

Sironi et al. (2013) (2013ApJ...771...54S)

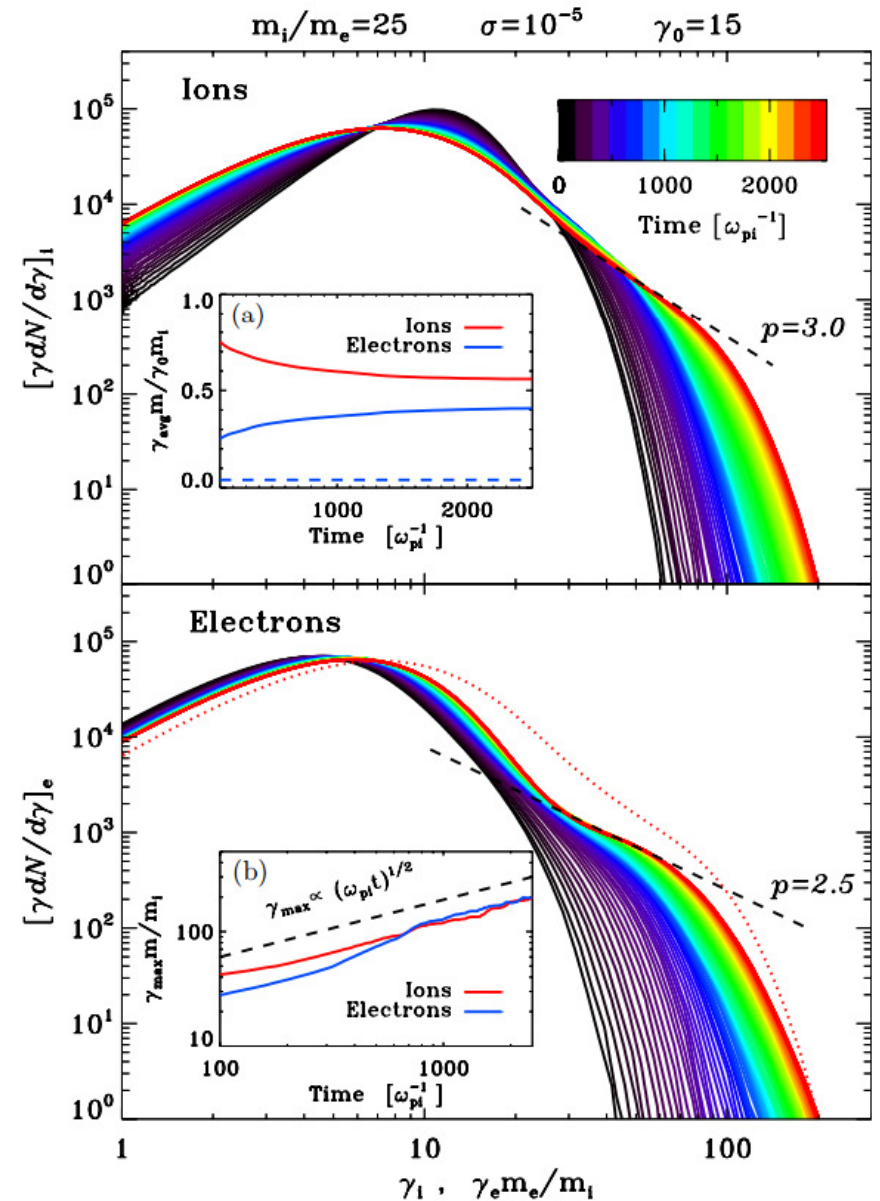
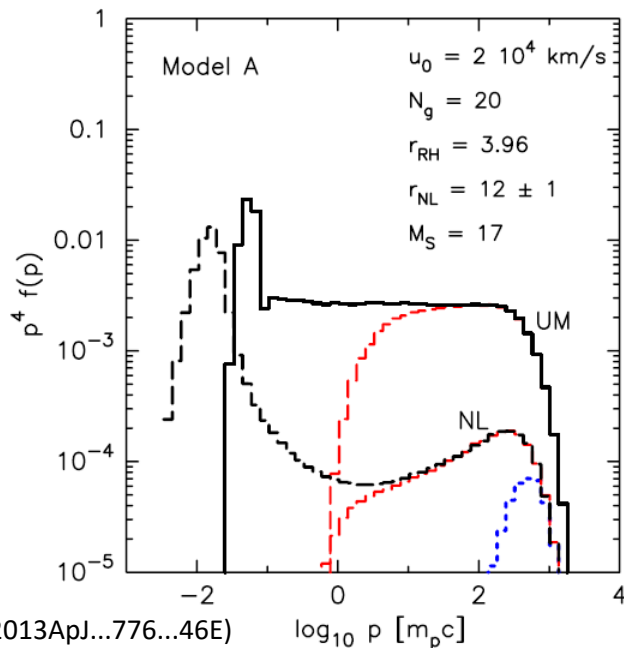


Figure 11. Temporal evolution of the post-shock particle spectrum, from the 2D simulation of a $\gamma_0 = 15$ electron-ion ($m_i/m_e = 25$) shock in a flow with magnetization $\sigma = 10^{-5}$.

Nonlinear DSA in relativistic shocks

Interaction between shock, B-field turbulence, and accelerated particles important!

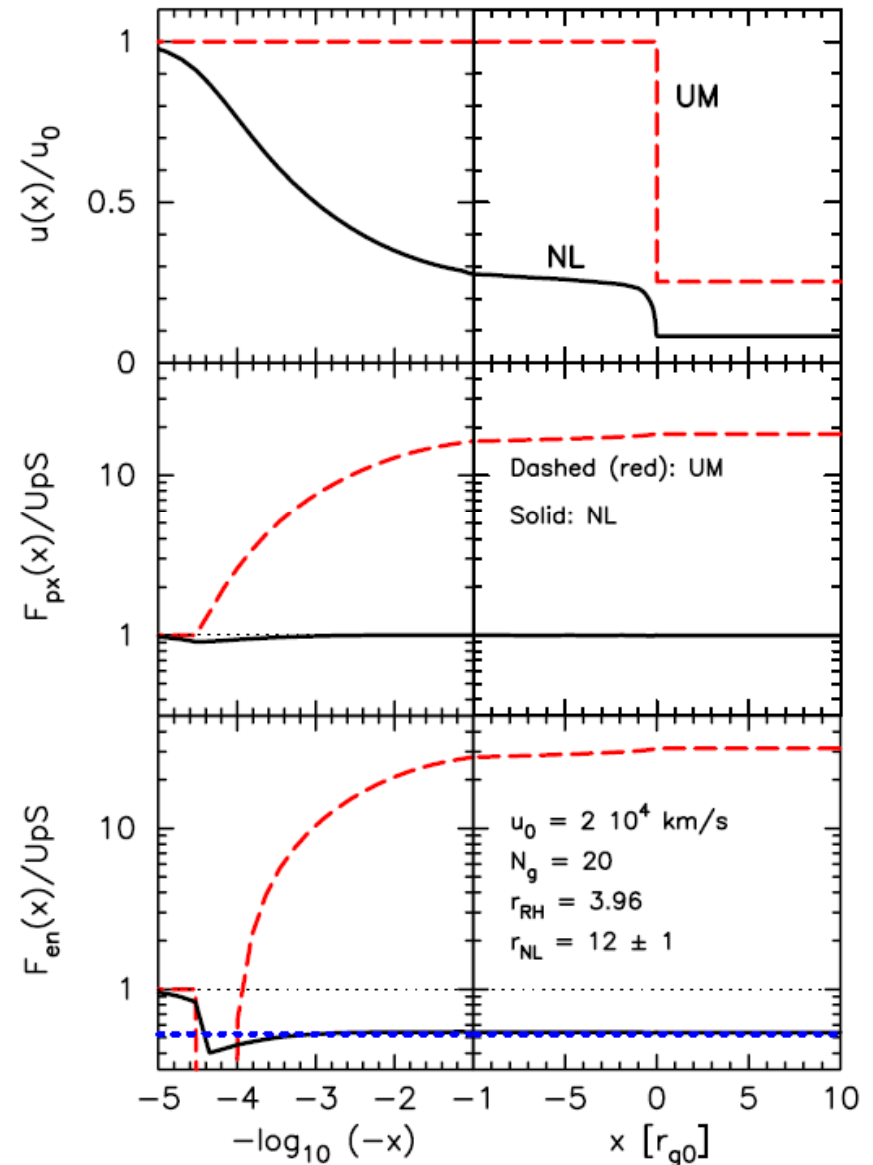
Efficient DSA by unmodified shocks does not conserve energy or momentum flux



Ellison et al. (2013) (2013ApJ...776...46E)

$\log_{10} p [m_p c]$

Ellison et al. (2013) (2013ApJ...776...46E)



Ellison et al. (2013) (2013ApJ...776...46E)

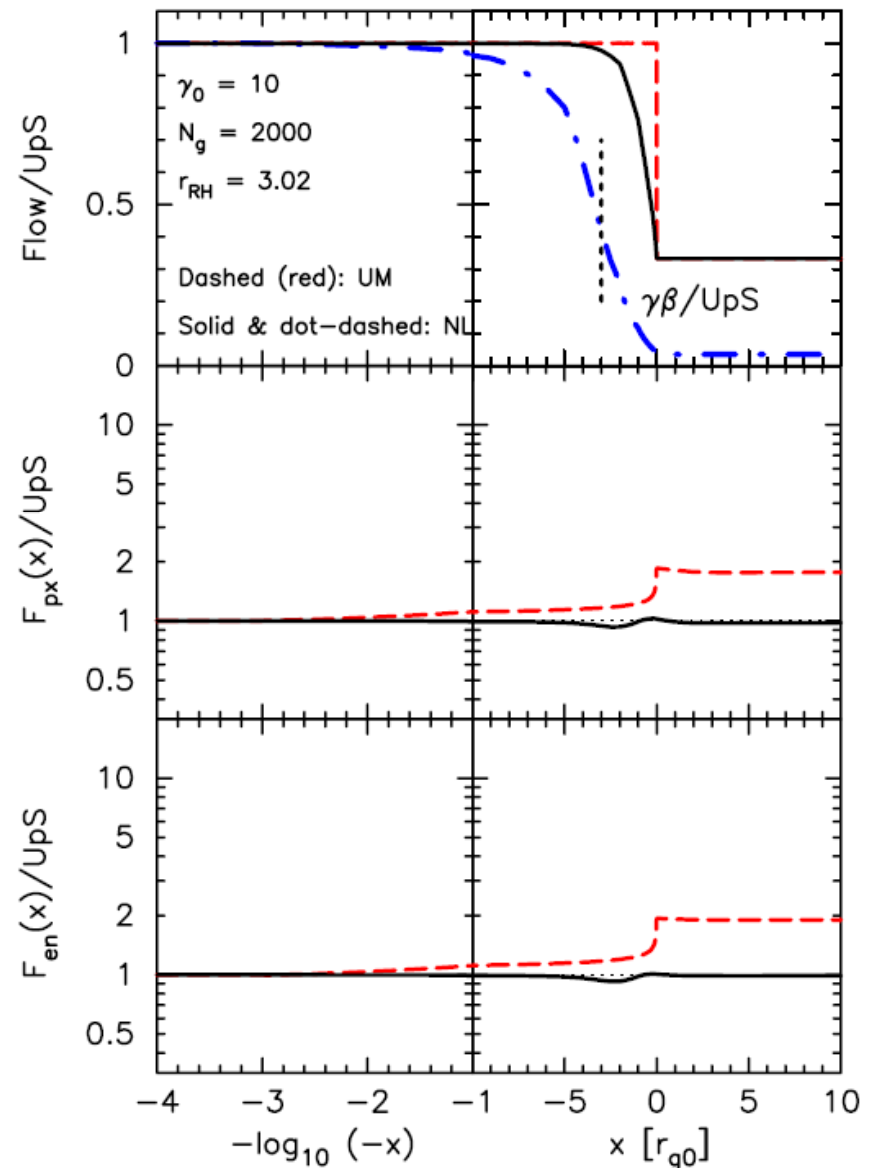
Nonlinear DSA in relativistic shocks

Interaction between shock, B-field turbulence, and accelerated particles important!

Efficient DSA by unmodified shocks does not conserve energy or momentum flux

Even in relativistic shocks, must have precursor & modified velocity profile

Ellison et al. (2013) (2013ApJ...776...46E)

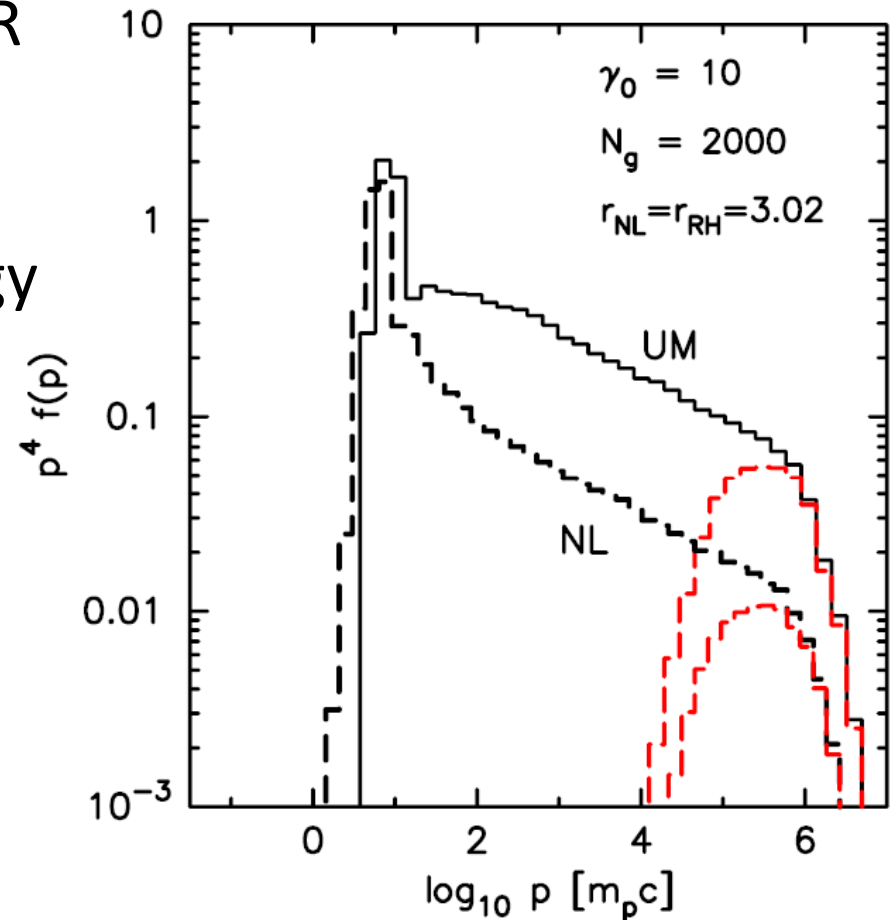


Nonlinear DSA in relativistic shocks

Ellison et al. (2013) (2013ApJ...776...46E)

Effects of NLDSA on spectrum of CR protons:

- Fewer CRs at any particular energy
- Region of steep decay before spectrum flattens to $\approx p^{-4.23}$
- Approx. 30% of energy in CRs, so acceleration still very efficient



Nonlinear DSA in relativistic shocks

As shock slows, CR spectrum changes too

Single-index approach to CR energy distribution may not hold at any given instant

Very unlikely to hold across extended observations of GRB afterglows

But what about electrons?

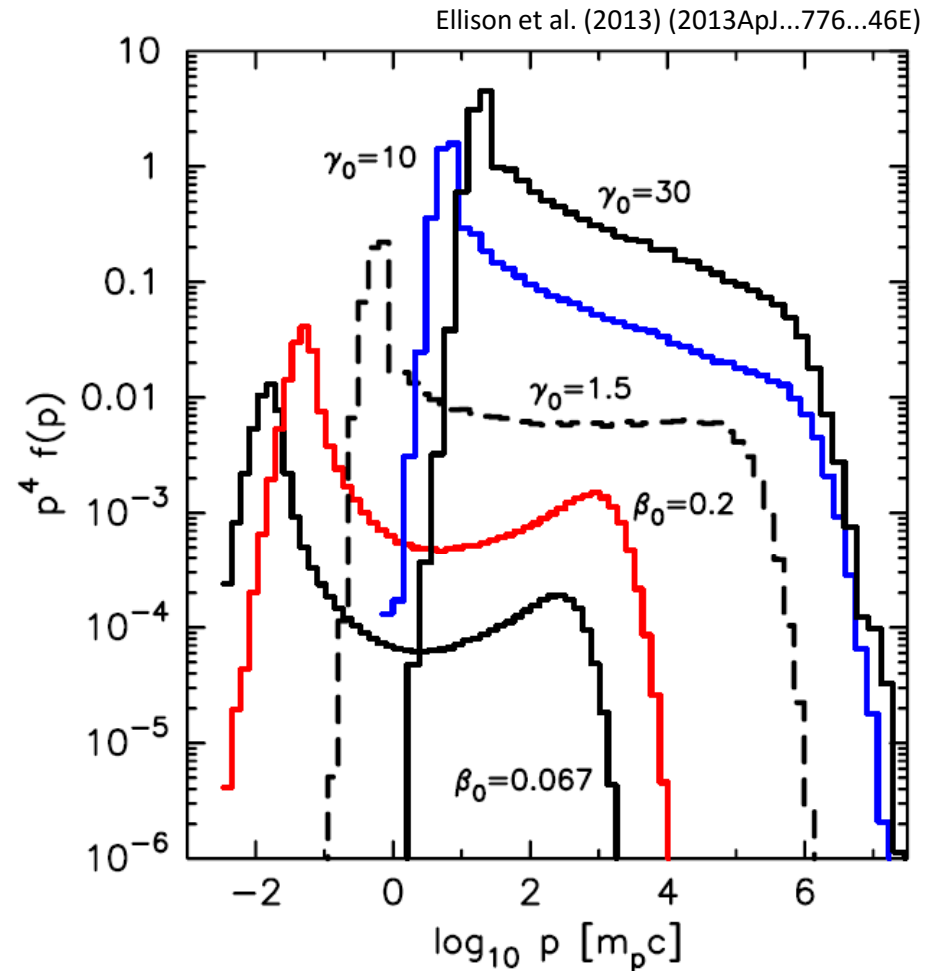


Figure 10. Nonlinear particle distributions calculated downstream from the shock in the shock rest frame for various shock speeds as indicated (Models A–E in Table 1). The spectrum for the $\gamma_0 = 1.5$ shock (dashed black curve) shows the transitional nature of nonlinear DSA.

Electron DSA in relativistic shocks

Warren et al. (2015) (2015MNRAS.452..431W)

Electron acceleration much less efficient than proton acceleration

Without energy transfer from ions, GRB afterglow would be extremely faint

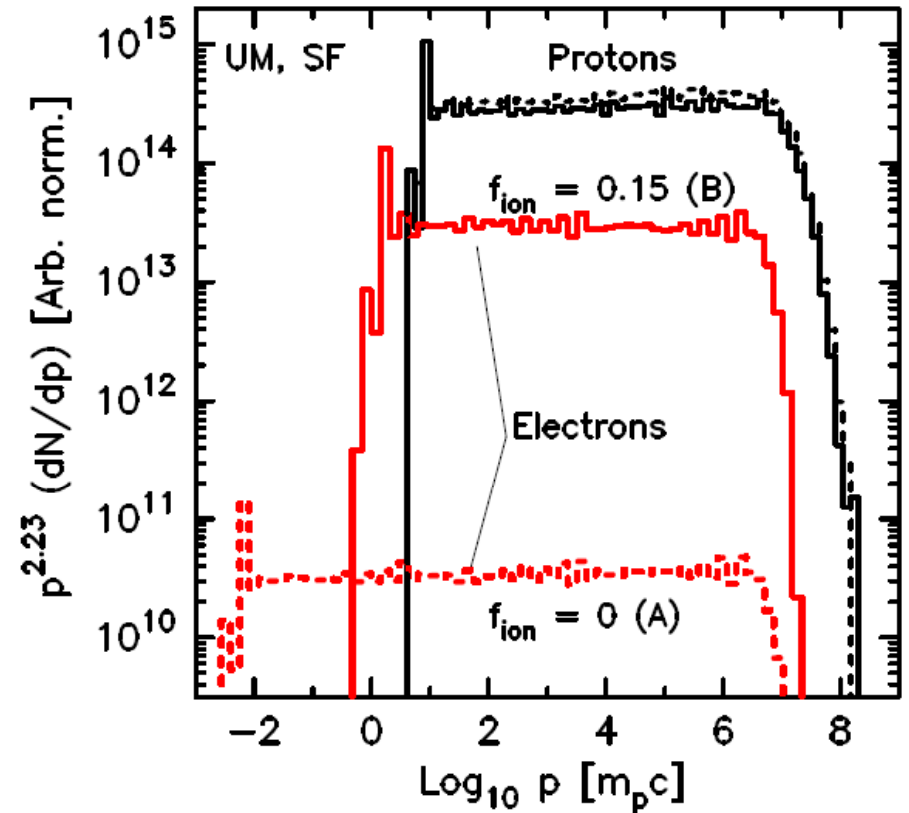


Figure 3. Protons (black curves) and electrons (red curves) from UM shocks with different f_{ion} as indicated. These spectra, multiplied by $p^{2.23}$, are calculated downstream from the shock, in the shock frame, and have arbitrary overall normalization although the relative normalization between electrons and protons is absolute.

Electron DSA in relativistic shocks

Sironi et al. (2013) (2013ApJ...771...54S)

Electron acceleration much less efficient than proton acceleration

Without energy transfer from ions, GRB afterglow would be extremely faint

PIC simulations (Sironi+ 2013, Ardaneh+ 2015) show that this transfer does occur

As much as 40% of bulk kinetic energy deposited into electrons

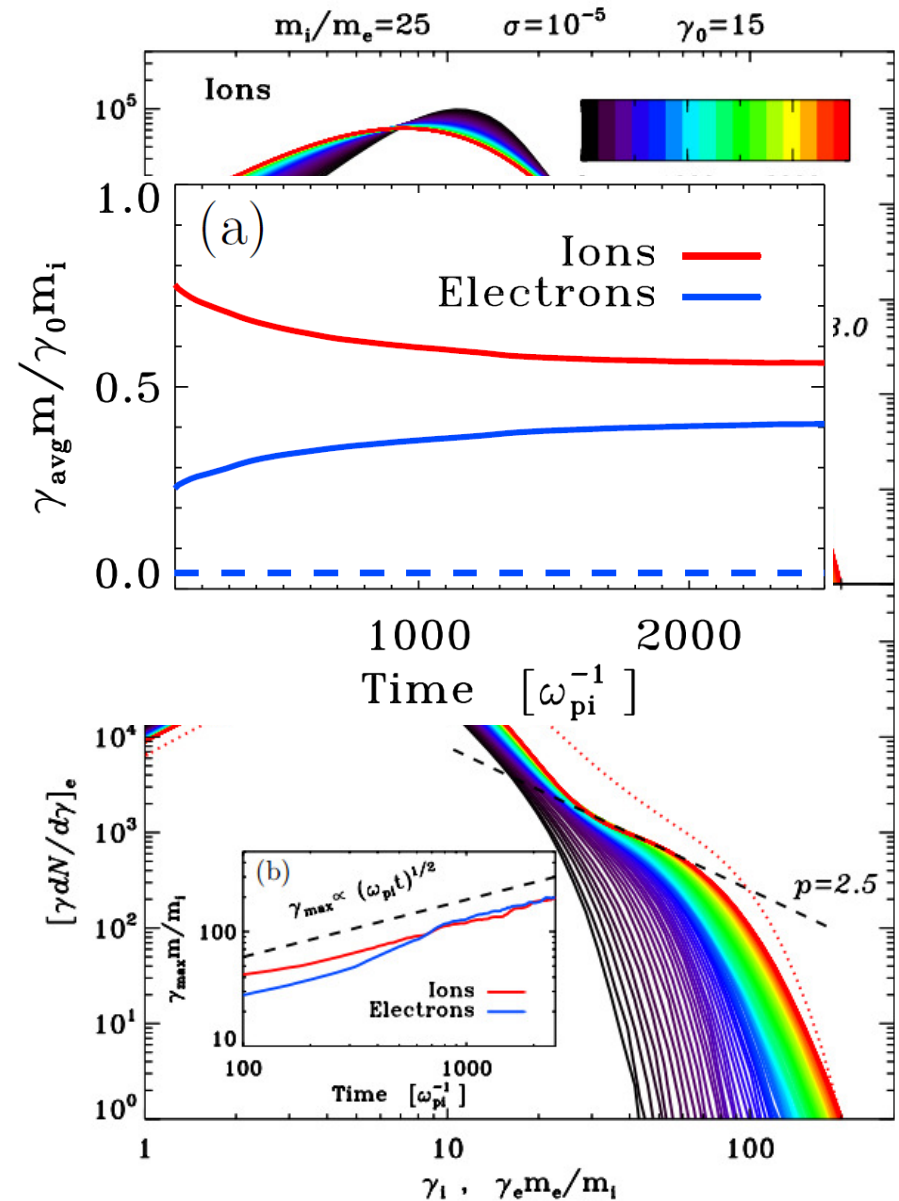


Figure 11. Temporal evolution of the post-shock particle spectrum, from the 2D simulation of a $\gamma_0 = 15$ electron-ion ($m_i/m_e = 25$) shock in a flow with magnetization $\sigma = 10^{-5}$.

Electron DSA in relativistic shocks

Warren et al. (2015) (2015MNRAS.452..431W)

Electron acceleration much less efficient than proton acceleration

Without energy transfer from ions, GRB afterglow would be extremely faint

Even 15% transfer causes 1000x increase in electron presence, but minimal change to protons

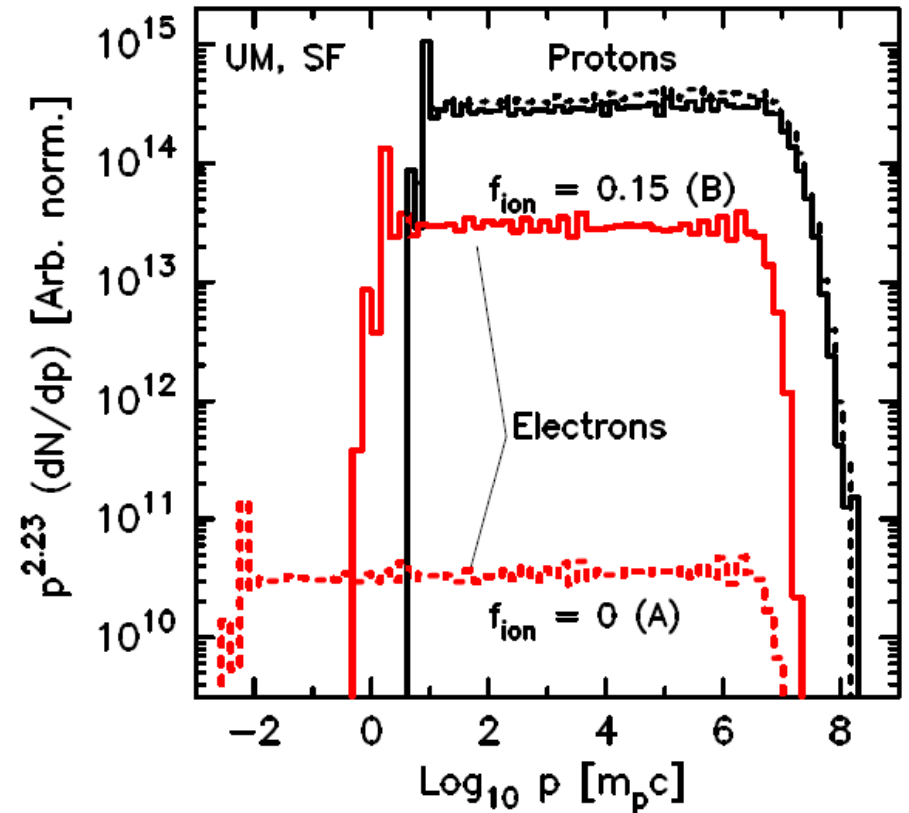


Figure 3. Protons (black curves) and electrons (red curves) from UM shocks with different f_{ion} as indicated. These spectra, multiplied by $p^{2.23}$, are calculated downstream from the shock, in the shock frame, and have arbitrary overall normalization although the relative normalization between electrons and protons is absolute.

Electron DSA in relativistic shocks

Ellison et al. (2013) (2013ApJ...776...46E)

For protons, not much difference between unmodified DSA and nonlinear DSA

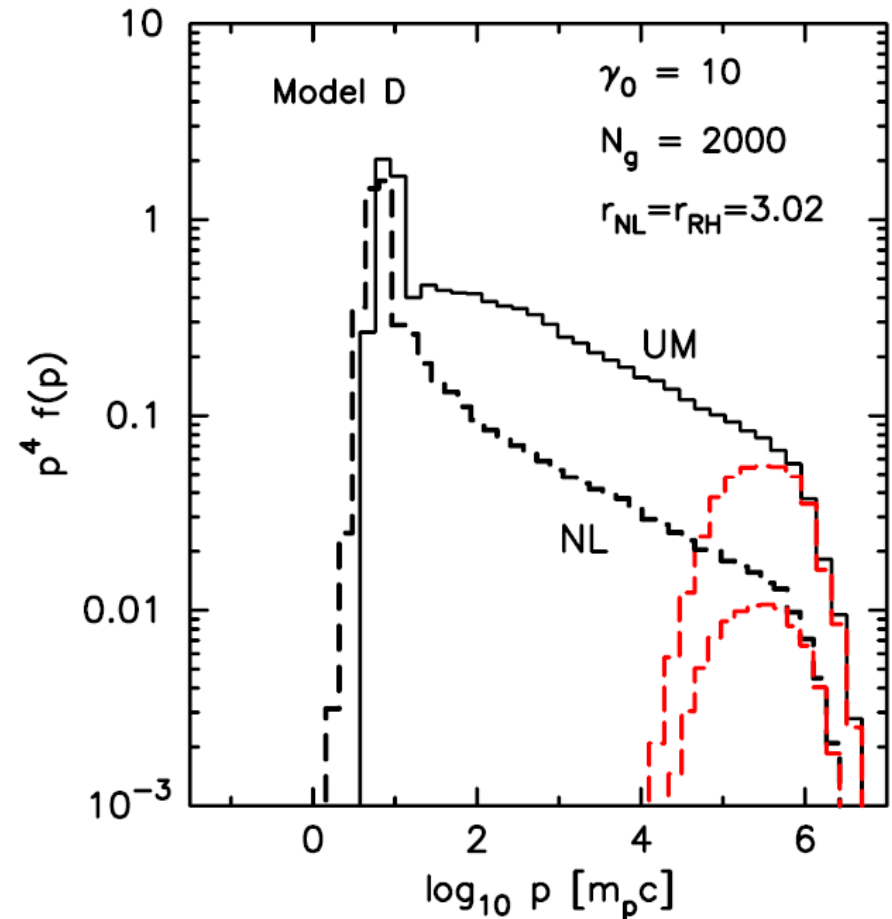


Figure 9. Comparison of UM shock spectrum (Model D; same as in Figure 3) with NL shock spectrum. The shock structures for these $\gamma_0 = 10$ shocks are shown in Figure 6. The solid (black curves) are calculated downstream from the subshock in the shock rest frame and the dashed (red) curves are calculated in the shock precursor at $x = -100r_{g0}$.

Electron DSA in relativistic shocks

Warren et al. (2015) (2015MNRAS.452..431W)

For protons, not much difference between unmodified DSA and nonlinear DSA

For electrons, difference is stark

- >100x fewer electron CRs at highest energies
- No clear power law in NL electron spectrum

10% energy transferred

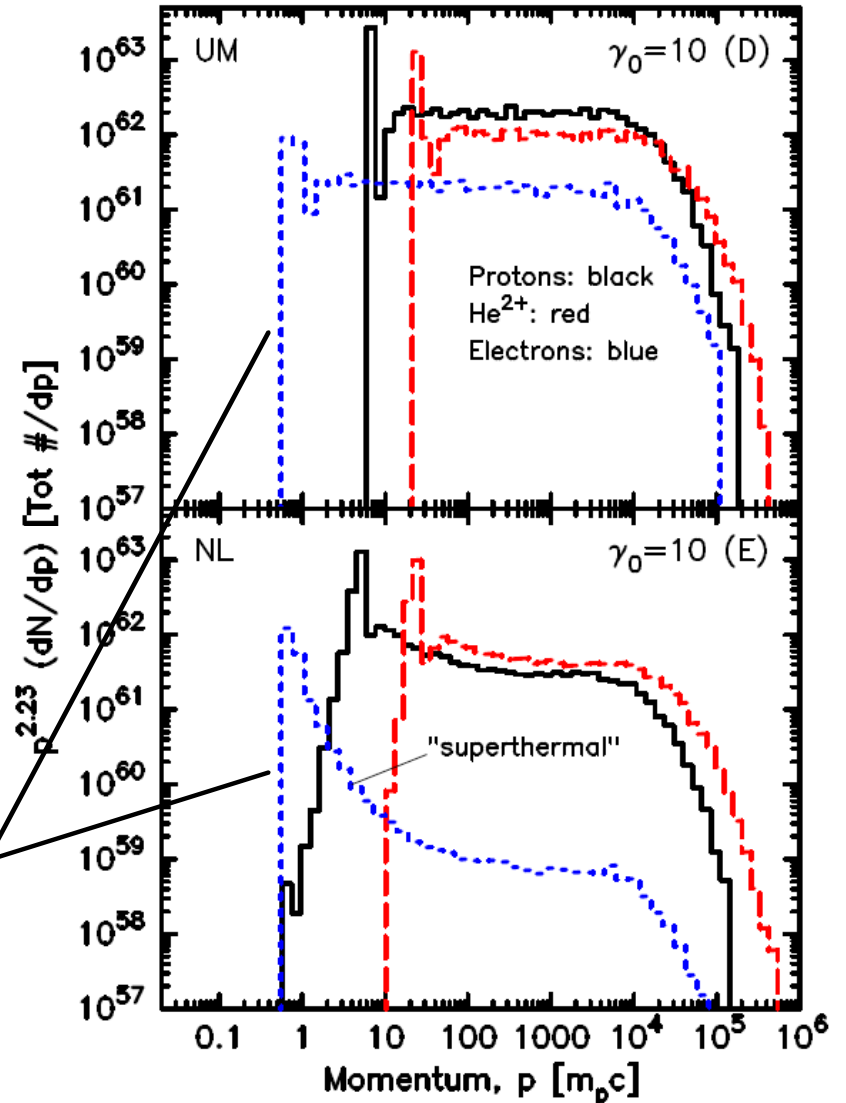


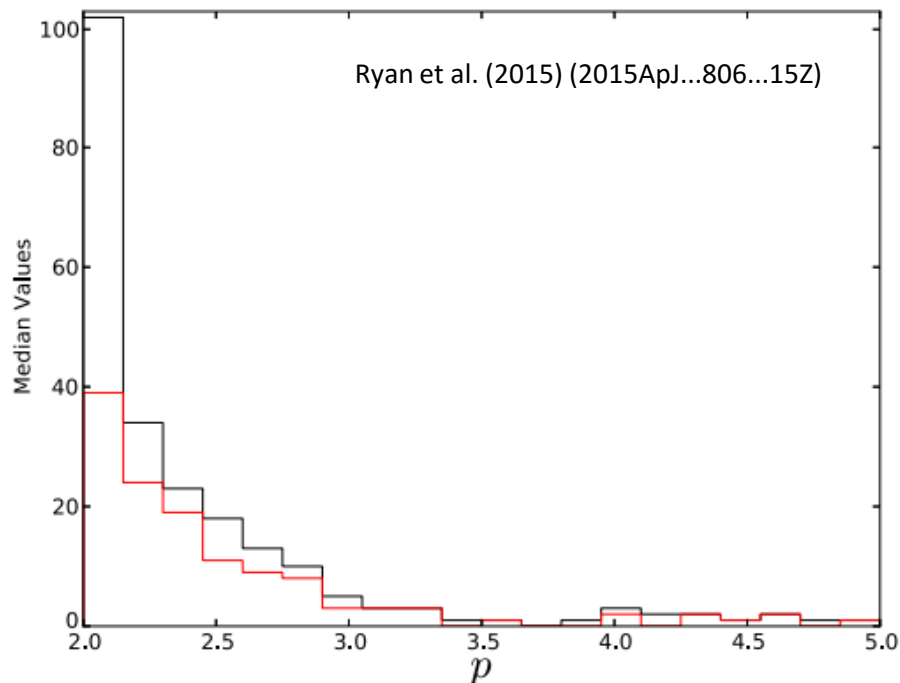
Figure 6. Downstream, LPF spectra for the unmodified shock shown in Fig. 5 (top panel, Model D) and the non-linear shock shown in Fig. 5 (bottom panel, Model E). Note the pronounced 'superthermal' tail on the electron distribution.

Electron DSA in relativistic shocks

Curran et al. (2010) (2010ApJ...716L.135C)

Model	p	σ_p
GDp	2.36	0.590
	(2.40 ± 0.03)	(0.600 ± 0.007)
	$[2.36 \pm 0.05]$	$[0.590 \pm 0.012]$

Notes. The most likely values of electron energy distribution index, p , the related Gaussian scatter, σ_p , the



Warren et al. (2015) (2015MNRAS.452..431W)

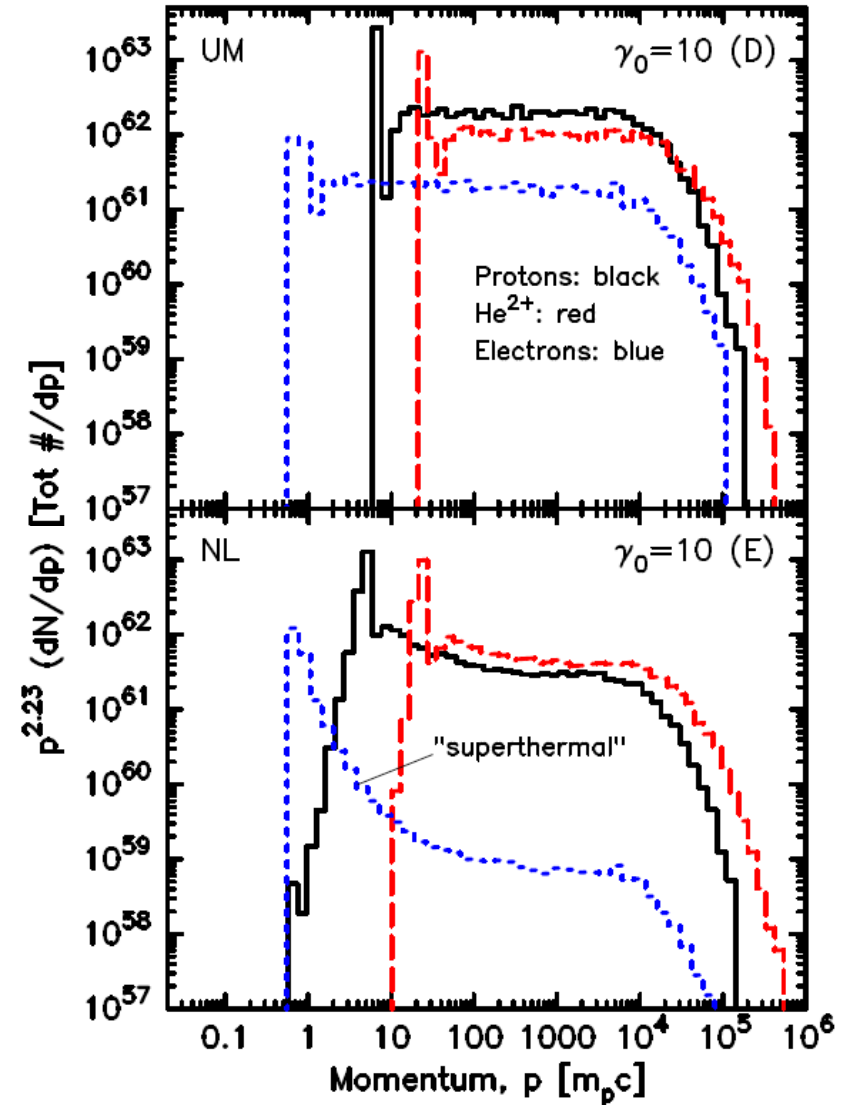


Figure 6. Downstream, LPF spectra for the unmodified shock shown in Fig. 5 (top panel, Model D) and the non-linear shock shown in Fig. 5 (bottom panel, Model E). Note the pronounced 'superthermal' tail on the electron distribution.

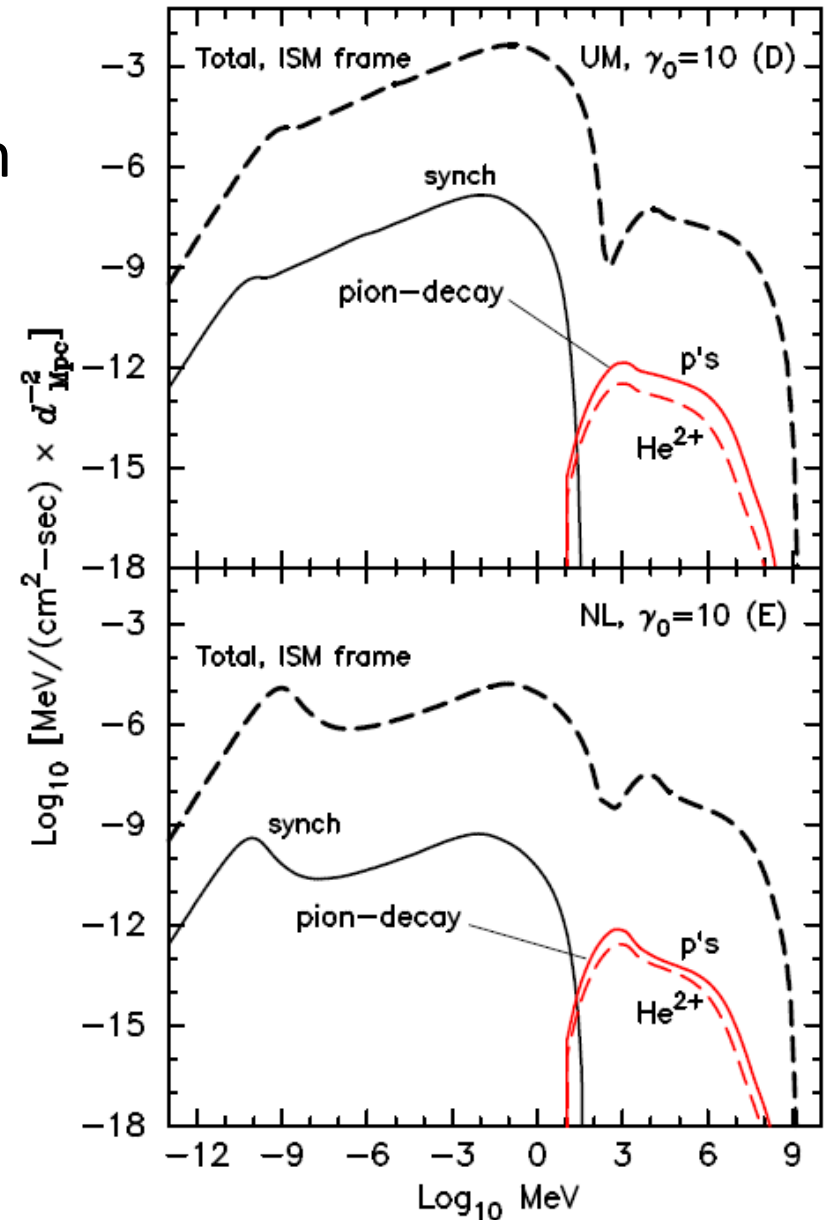
Electron DSA in relativistic shocks

Difference in electron spectrum visible in broadband photon spectrum as well

Thermal peak in synchrotron (from non-CR electrons) strongly enhanced in nonlinear model

However: Weibel instability shuts off around $\gamma_0 \approx 10$, so less/no energy transfer?

Warren et al. (2015) (2015MNRAS.452..431W)



Modeling a GRB afterglow

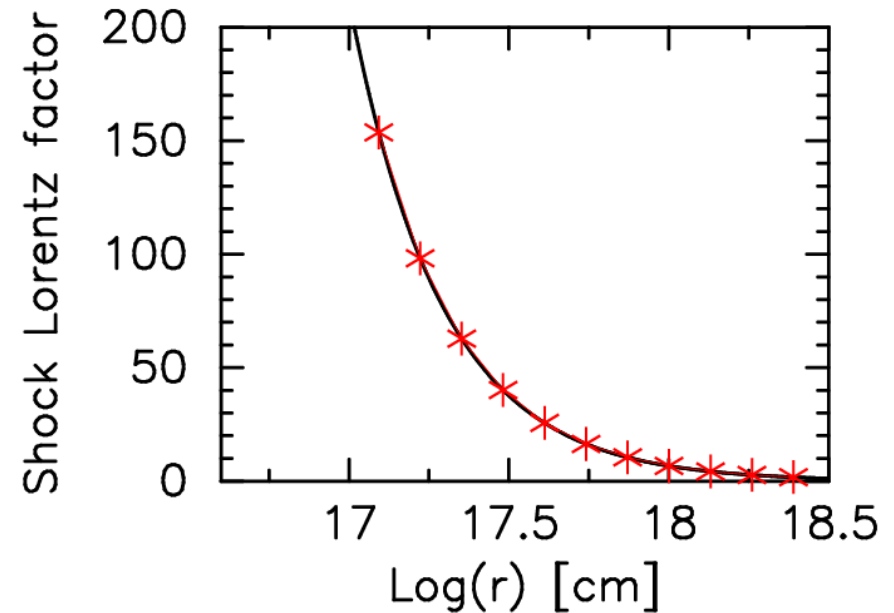
Use Blandford—McKee solution for hydrodynamical base

At select times, model nonlinear DSA process using Monte Carlo code

Calculate photon spectra

Two models discussed here:

- Far upstream B field of $3 \mu\text{G}$
- Far upstream B field of 3 mG

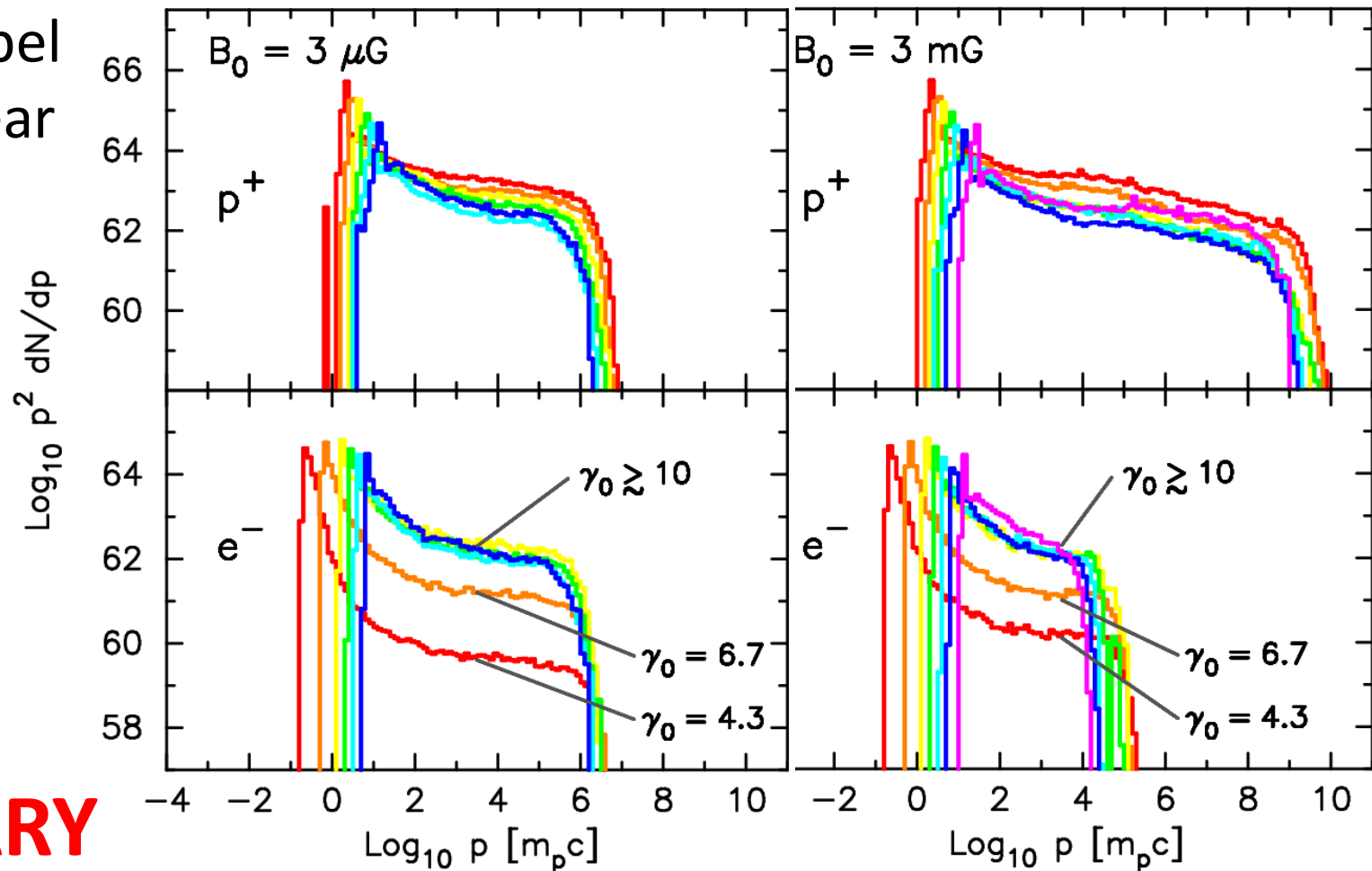


**EVERYTHING
PRELIMINARY**

Modeling a GRB afterglow

Stronger magnetic field increases p^+ max energy, decreases e^- max energy

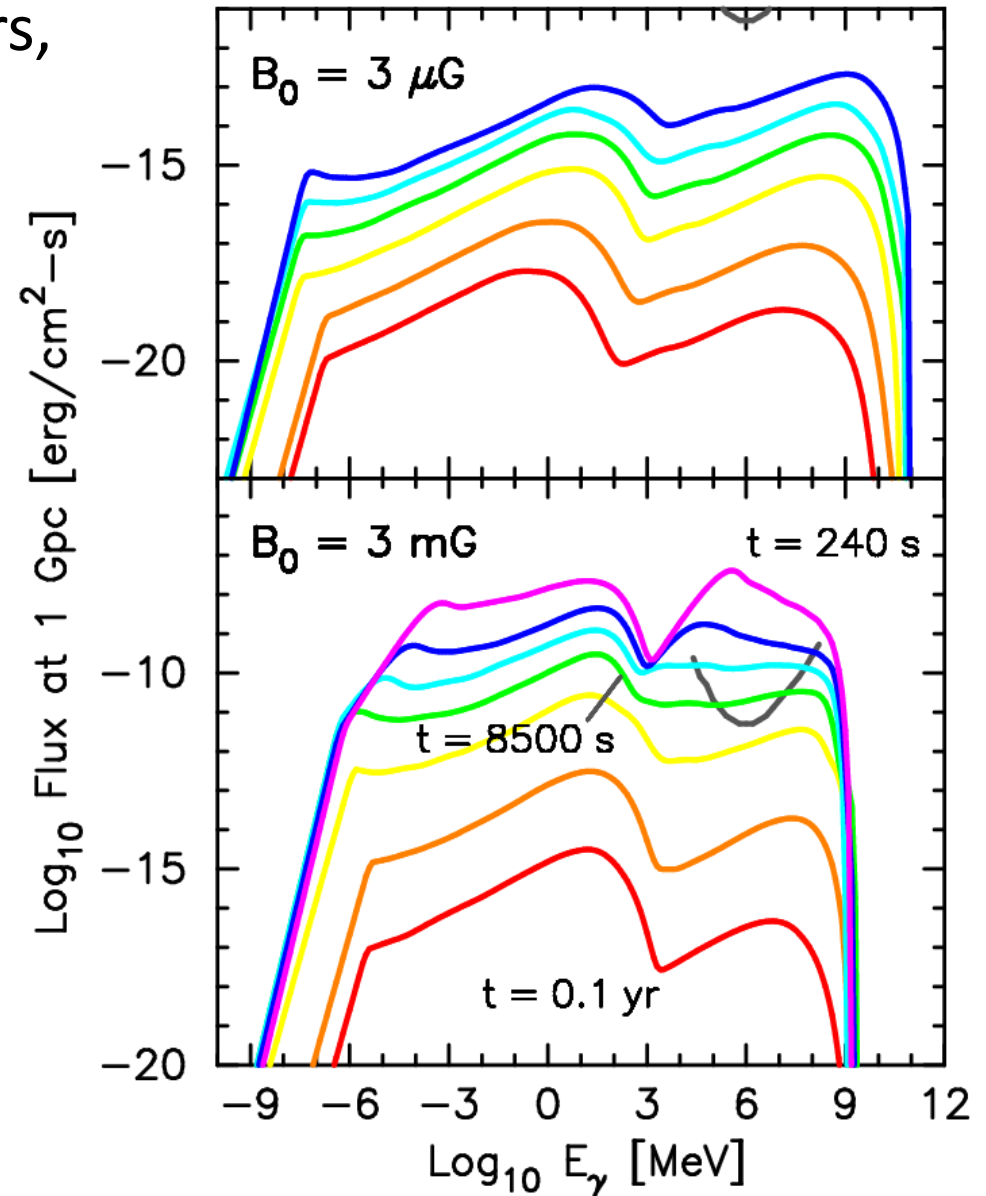
Shutoff of Weibel instability is clear from late-time e^- spectra



PRELIMINARY

Modeling a GRB afterglow

- For typical afterglow parameters, high-energy part of spectrum may be observable for $\approx 10^4$ s after GRB
- Detection or non-detection could serve as probe of micro-physics at shock front (e.g. strength of turbulent field, decay scale of turbulence)



PRELIMINARY

Conclusions

If CR acceleration by relativistic shocks efficient, **must** consider nonlinear interaction between shock & CRs

Shape of electron spectrum strongly affected by energy transfer & shock speed

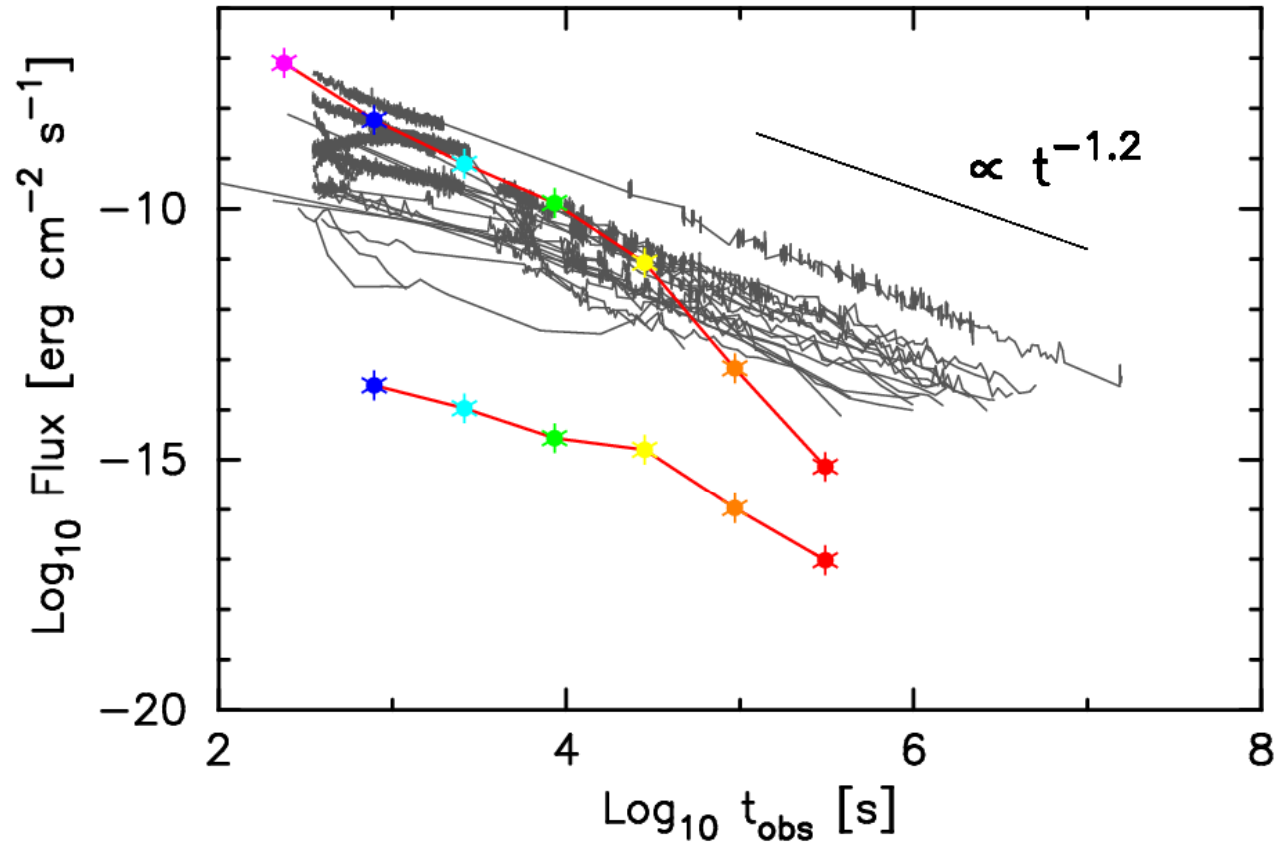
Single-value models of GRB afterglows highly likely to be deficient. Combining entire afterglow into one p , ϵ_B , ϵ_e , etc. misses a great deal of structure

With CTA, can (hopefully) observe early phase of afterglow in great detail to test theories of relativistic shocks and diffusive shock acceleration

Bonus slides

Low- B_0 model fails to reproduce observed X-ray fluxes; high- B_0 model *overproduces* at early times

Spectral break at $\approx 10^4$ s due to shutoff of Weibel instability when $\gamma_0 < 10$; it is *not* a jet break, but does occur at same time



PRELIMINARY